

Photocatalytic Oxidation of Alcohols over TiO₂ Covered with Nb₂O₅

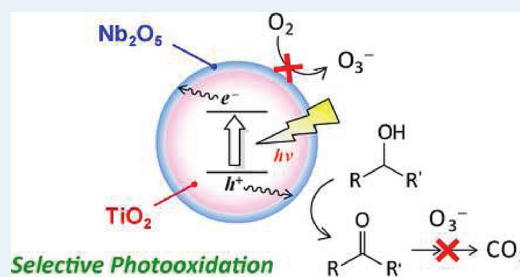
Shinya Furukawa, Tetsuya Shishido,* Kentaro Teramura, and Tsunehiro Tanaka*

Department of Molecular Engineering, Graduate School of Engineering, Kyoto University, Kyoto 615-8510, Japan

Supporting Information

ABSTRACT: A selectivity enhancement in alcohol photooxidation using TiO₂ covered with Nb₂O₅ is demonstrated. A series of TiO₂ covered with Nb₂O₅ catalysts (Nb₂O₅/TiO₂, loading of Nb₂O₅; 0–5 mol %) were prepared and characterized. XPS studies suggest that the TiO₂ surface was completely covered with Nb₂O₅ at a 3.5 mol % loading. UV–vis spectra of TiO₂ and the Nb₂O₅/TiO₂ series revealed that the band gap energy of the catalyst was not changed upon addition of Nb₂O₅. The amounts of photogenerated oxygen anion radical species (O₂^{•-} and O₃^{•-}) over the catalyst, as estimated by ESR, drastically decreased with increased loadings of Nb₂O₅. The O₃^{•-} anion, in particular, which can be formed on anatase TiO₂, completely disappeared at Nb₂O₅ loadings over 4 mol %. In the oxidations of several alcohols (1-pentanol, 2-pentanol, 3-pentanol, and cyclohexanol), the Nb₂O₅/TiO₂ catalysts exhibited higher selectivities than TiO₂ with comparable conversion levels. Furthermore, the Nb₂O₅/TiO₂ system gave a higher photocatalytic activity compared with Nb₂O₅ without lowering the selectivity.

KEYWORDS: surface coverage, monolayer, titanium oxide, niobium oxide, alcohol photooxidation



INTRODUCTION

Heterogeneous photocatalysis has a potential application in the aerobic oxidation of organic molecules.^{1–3} Numerous semiconductor-type metal oxides have been tested as photocatalysts for oxidation, but it is generally accepted that anatase TiO₂ is the most reliable material due to its low cost, high photostability, and photocatalytic activity. Recently, much effort has been devoted to the application of TiO₂ to the selective catalytic oxidation of alkanes^{4–7} and alcohols,^{8–15} however, undesired overoxidation to carbon dioxide (CO₂) is essentially associated with the photocatalytic oxidation over TiO₂ due to the presence of highly oxidizing radical species: positive holes trapped by surface lattice oxygen (O⁻),^{16,17} ozonide ion (O₃⁻),^{18,19} or the hydroxyl radical (HO•).² It is generally accepted that O₃⁻ is formed upon the combination of O⁻ and O₂^{18–20} and that HO• is released via the oxidation of a surface hydroxyl group by a hole.^{2,21} Tsukamoto et al. reported that TiO₂ partially coated with WO₃ showed higher activity and selectivity in the photooxidation of benzylic alcohols to aldehydes than TiO₂ under diluted conditions (5 mg of catalyst, 0.1 mmol of alcohol, and 5 mL of water as a solvent).²² They interpret that the phenomena that TiO₂ surface of the catalyst, which is active for oxidation, is partially coated with WO₃ layer (WO₃ loading: 7.6 wt %), which leads to a decrease in the amount of aldehyde adsorbed on the TiO₂ surface. It appeared that the area of TiO₂ surface was decreased by WO₃ addition. However, not only the selectivity to aldehyde but also the rate of alcohol conversion increased. Therefore, it seems that the WO₃ layer has another role in addition to the adsorption site of photogenerated aldehyde.

We reported that the selective photooxidation of alcohols proceeded over niobium oxide (Nb₂O₅) and showed a higher

selectivity than TiO₂ with a comparable conversion level.²³ ESR studies suggested that this high selectivity was due to the absence of O₃⁻ over Nb₂O₅, in contrast to TiO₂ under photo irradiation;²⁴ however, the photocatalytic activity of Nb₂O₅ in the oxidation of alcohols was much lower than that of TiO₂. To develop an effective photocatalyst that exhibits both high activity and selectivity in the aerobic oxidation of alcohols, there are two primary strategies: improve the photocatalytic activity of Nb₂O₅ or enhance the selectivity of TiO₂. In the first strategy, we have already achieved a remarkable increase in photocatalytic activity by addition of Cu to Nb₂O₅.²⁵ In the oxidation of alcohols over Cu/Nb₂O₅, the Cu(I) site operates as a desorption site and successfully promotes the desorption of the produced carbonyl compound, which is the rate-determining step.²⁶ In the latter, attention should be focused on how the formation of the highly oxidizing species above-mentioned is inhibited. In this context, a promising approach is to cover the surface of TiO₂ with Nb₂O₅, which inhibits the production of highly oxidizing O₃⁻ (Scheme 1).

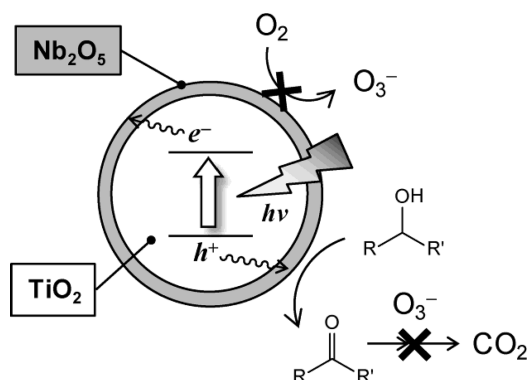
In this study, we have prepared a series of TiO₂ covered with Nb₂O₅ photocatalysts and their photocatalytic activities and selectivities have been compared with those of bare TiO₂ or Nb₂O₅ in the oxidation of alcohols. The correlation between the amount of photogenerated oxygen anion radicals and selectivity has also been investigated. Here in, we demonstrate that it is effective for selective oxidation using TiO₂-based photocatalysts to inhibit the formation of O₃⁻ by surface coverage of TiO₂.

Received: October 26, 2011

Revised: December 15, 2011

Published: December 16, 2011

Scheme 1. Strategy for the Selective Photocatalytic Oxidation of Alcohols over $\text{Nb}_2\text{O}_5/\text{TiO}_2$ ^a



^aThe inhibition of O_3^- generation by surface coverage of TiO_2 with Nb_2O_5 is shown.

EXPERIMENTAL SECTION

Catalyst Preparation. Ammonium niobium oxalate ($\text{NH}_4[\text{NbO}(\text{C}_2\text{O}_4)_2(\text{H}_2\text{O})] \cdot n\text{H}_2\text{O}$), as a precursor of niobium oxide, and niobium oxide hydrate ($\text{Nb}_2\text{O}_5 \cdot n\text{H}_2\text{O}$, HY-340) were kindly supplied by CBMM (Araxa, Brazil). The TiO_2 sample used in this study, JRC-TIO-4 (equivalent to Degussa. P-25; rutile/anatase = 3/7; BET surface area = $49 \text{ m}^2 \cdot \text{g}^{-1}$) was supplied by the Japan Catalysis Society. After the hydration of TiO_2 in distilled water for 2 h at 353 K and evaporation at 368 K, the sample was dried at 353 K overnight. The TiO_2 catalyst was then calcined in dry air at 773 K for 5 h. A series of TiO_2 supported niobium oxide catalysts ($n \text{ mol } \% \text{ Nb}_2\text{O}_5/\text{TiO}_2$; $n = 1-5$) were prepared by impregnation of the TiO_2 sample with aqueous solutions of ammonium niobium oxalate followed by calcination at 773 K for 5 h. Nb_2O_5 catalyst (BET surface area = $48 \text{ m}^2 \cdot \text{g}^{-1}$)²³ was prepared by calcination of niobium oxide hydrate in a dry air flow at 773 K for 5 h. All catalysts were ground into powders under a 100 mesh (0.15 mm) after calcination.

Characterization. A Rigaku MultiFlex DR Powder X-ray diffractometer (XRD) was used for the identification of compounds formed on the catalyst samples. Specific surface areas were evaluated using the BET method using liquid nitrogen with a BEL Japan BELSORP28 28A. UV-vis diffuse reflectance spectra (1 nm resolution) were obtained with a JASCO UV570 spectrometer. X-ray photoelectron spectra (XPS) were acquired using an ULVAC PHI 5500MT. XPS samples were mounted on an indium foil, and the spectra were measured using $\text{Mg K}\alpha$ radiation (15 kV, 400 W) in a chamber with the base pressure of $\sim 10^{-9}$ Torr. The takeoff angle was set at 45° . Binding energies were referenced to the O 1s level at 530.2 eV.

ESR Measurement of Oxygen Anion Radicals. ESR measurements were carried out using an X-band ESR spectrometer (JEOL JES-SRE2X) with an in situ quartz cell. Prior to ESR measurement, the sample was pretreated with 6.7 kPa O_2 at 673 K for 1 h, followed by evacuation for 0.5 h at 673 K. After pretreatment, the sample was exposed to 0.5 kPa O_2 at room temperature. The sample was then cooled to 123 K and irradiated. ESR spectra were recorded before and after photoirradiation at 123 K. The g values and the amounts of yielded radical species were determined using a certain amount of Mn/MgO marker. The radical amounts of the Mn/MgO marker were determined using 4-hydroxy-2,2,6,6-tetramethylpi-

peridine-1-oxyl (TEMPOL; radical density 97%, purchased from Wako). A 500 W ultrahigh-pressure mercury lamp was used as a light source.

Reaction Conditions. The photocatalytic oxidations of alcohols were carried out in a quasi-flowing batch system²⁵ (see Supporting Information, Figure S1) under atmospheric oxygen. The catalyst (100 mg), alcohol (10 mL), and a stirrer bar were introduced to a Pyrex glass reactor. No solvent was used. The substrate was used without further purification. The suspension was vigorously stirred at room temperature and irradiated from the flat bottom of the reactor via reflection using a cold mirror with a 500 W ultrahigh-pressure Hg lamp (USHIO Denki Co.). Oxygen was flowed into the reactor at $2 \text{ cm}^3 \cdot \text{min}^{-1}$. Organic products were analyzed by FID-GC (Shimadzu GC-14B) and GC-MS (Shimadzu GC-MS QP5050). At the down stream of the flow reactor, a saturated barium hydroxide solution ($\text{Ba}(\text{OH})_2$) was set up to determine the quantities of carbon dioxide (CO_2) formed as barium carbonate (BaCO_3). The partial oxidation product selectivities are defined as yields (mmol) of aldehyde and acid (partial oxidation products) per yield (mmol) of aldehyde, acid and $1/n \text{ CO}_2$ (n = the number of carbon atoms of the substrate).

RESULTS AND DISCUSSION

Characterization of Catalysts. The valences of niobium and titanium cations in a few atomic layers of the $\text{Nb}_2\text{O}_5/\text{TiO}_2$ catalyst surface were evaluated using XPS. The binding energies of the Nb 3d and Ti 2p peaks of $\text{Nb}_2\text{O}_5/\text{TiO}_2$ did not change, regardless of Nb_2O_5 loading (Figure S2 of the Supporting Information). These Nb 3d (207.1 eV for $3d_{5/2}$ and 209.8 eV for $3d_{3/2}$) and Ti 2p (464.5 eV for $2p_{3/2}$ and 458.8 eV for $2p_{1/2}$) peaks can be assigned to Nb^{5+} and Ti^{4+} , respectively. The Nb/Ti ratios in a few atomic layers of the $\text{Nb}_2\text{O}_5/\text{TiO}_2$ catalyst surface were estimated from the areas of Nb 3d and Ti 2p XPS, as shown in Figure 1. The Nb/Ti ratio increases linearly with

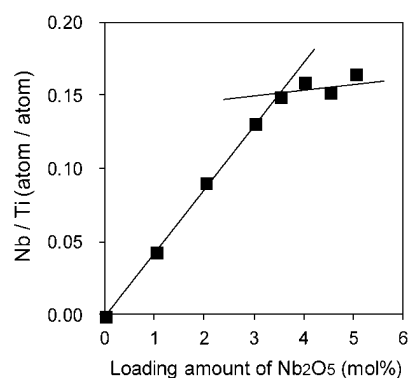


Figure 1. Changes in surface Nb/Ti ratio with Nb_2O_5 loading.

increasing Nb_2O_5 loading up to 3.5 mol % (equivalent to 10 wt %). It then becomes more gradual. The linear relationship indicates the formation of a two-dimensional niobium oxide overlayer, and the change in the slope can be attributed to the transition from a two-dimensional overlayer to three-dimensional particles (monolayer coverage) at loadings over 3.5 mol % Nb_2O_5 .²⁷

The XRD patterns of a series of $\text{Nb}_2\text{O}_5/\text{TiO}_2$ catalysts were compared with those of TiO_2 and Nb_2O_5 , as shown in Figure 2. The patterns for 1–4 mol % $\text{Nb}_2\text{O}_5/\text{TiO}_2$ samples indicate no changes in the crystallinity of the TiO_2 support (anatase and

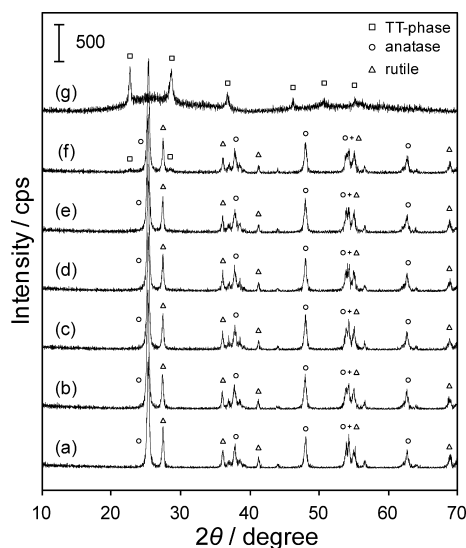


Figure 2. XRD patterns of (a) TiO_2 ; (b) 1, (c) 2, (d) 3, (e) 4, and (f) 5 mol % $\text{Nb}_2\text{O}_5/\text{TiO}_2$; and (g) Nb_2O_5 .

rutile) and no formation of a niobium oxide crystallite. On the other hand, the 5 mol % $\text{Nb}_2\text{O}_5/\text{TiO}_2$ exhibits a small feature assignable to TT- Nb_2O_5 ,^{28–31} which is associated with TiO_2 . Similar diffraction patterns have also been reported for 7.7³² or 11³³ mol % $\text{Nb}_2\text{O}_5/\text{TiO}_2$ samples. The formation of a niobium oxide crystallite at loadings over 3.5 mol % is consistent with the results from the XPS study. UV–vis spectra of the 1–5 mol % $\text{Nb}_2\text{O}_5/\text{TiO}_2$ catalysts were also identical to that of TiO_2 (Supporting Information Figure S3), whose band gap energy was estimated as 3.10 eV. The Nb_2O_5 catalyst possesses spectral features similar to that of TiO_2 , and the band gap energy was estimated as 3.16 eV (Supporting Information Figure S3). Thus, the surface coverage of TiO_2 with Nb_2O_5 does not influence the crystallinity of the TiO_2 support and does not change the optical properties of the catalysts. The BET surface area measurements revealed that the surface area of TiO_2 ($49 \text{ m}^2 \cdot \text{g}^{-1}$) was maintained after the addition of Nb_2O_5 (Supporting Information Figure S4).

ESR Measurements of Photogenerated Oxygen Anion Radicals. We characterized the photogenerated oxygen anion radical species over TiO_2 , $\text{Nb}_2\text{O}_5/\text{TiO}_2$, and Nb_2O_5 using ESR and estimated the amounts of the radical species. Figure 3

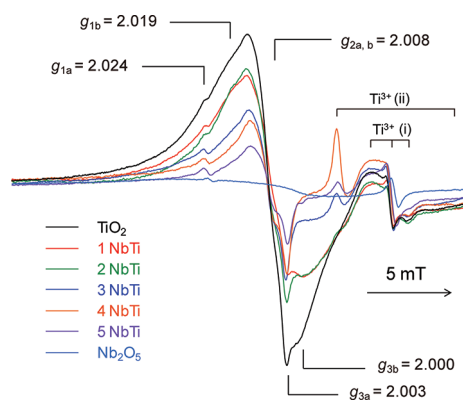


Figure 3. ESR spectra of the photogenerated oxygen anion radical at 77 K over TiO_2 , n mol % $\text{Nb}_2\text{O}_5/\text{TiO}_2$ (abbreviated as $n\text{NbTi}$; $n = 1, 3, 5$), and Nb_2O_5 .

shows the ESR spectra obtained when the catalysts were irradiated in the presence of oxygen at 123 K. An intense signal consisting of two sets of rhombic g values were observed over TiO_2 , which can be assigned to superoxide (O_2^- : $g_1 = 2.024$, $g_2 = 2.009$, $g_3 = 2.003$)^{34–36} and ozonide (O_3^- : $g_1 = 2.019$, $g_2 = 2.006$, $g_3 = 2.000$).^{35–38} Such radical species over TiO_2 are well-known and have been widely characterized. Generally, it is proposed that the O_2^- is generated via the reduction of adsorbed O_2 by excited electrons. The O_3^- is formed from the combination of a positive hole captured by surface lattice oxygen (equivalent to O^-) and O_2 .^{20,35,39,40} In contrast, only a small broad signal was observed over Nb_2O_5 . In this case, using ^{17}O -enriched O_2 (20%) instead of $^{16}\text{O}_2$, a signal appeared with hyperfine splitting, as derived from the ^{17}O nuclei ($I = 5/2$) (Supporting Information Figure S5). This hyperfine structure indicates the generation of $^{16}\text{O}^{17}\text{O}^-$ and suggests that the two oxygen nuclei are equivalent. The equivalent hyperfine interactions are also consistent with the O_2^- ion being adsorbed in a side-on fashion onto the Nb_2O_5 surface, with its internuclear axis parallel to the plane of the surface. This type of adsorption is commonly observed with other metal oxides.²⁰ Eleven lines corresponding to the two ^{17}O nuclei ($^{17}\text{O}^{17}\text{O}^-$, $I = 5$) were expected, but apparently not observed, which is likely due to an inadequate enrichment of ^{17}O (20%).

The intensities of the ESR signals for the oxygen anion radicals were dramatically decreased with increasing of Nb_2O_5 loading. Although the signals assigned to O_2^- remained at a 5 mol % loading, the signal assigned to O_3^- completely disappeared at loadings over 4 mol %. This result strongly indicates that the TiO_2 surface, which can produce O_3^- , is completely covered at loadings over 4 mol %. It is also consistent with a monolayer coverage at 3.5 mol % loading, as estimated from the XPS study. The amounts of photogenerated oxygen anion radical species are shown in Figure 4. The

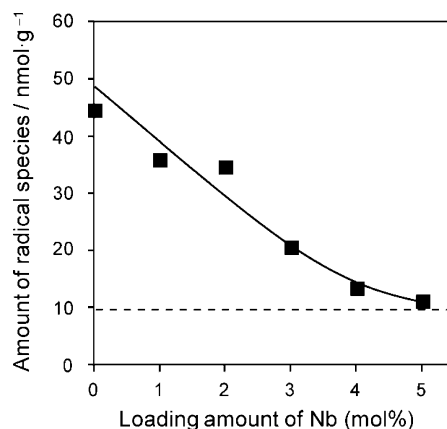
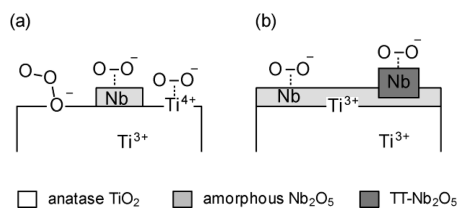


Figure 4. Changes in the amount of photogenerated oxygen anion radical species ($\text{O}_2^- + \text{O}_3^-$) over $\text{Nb}_2\text{O}_5/\text{TiO}_2$ catalyst with Nb_2O_5 loading. The dotted line shows the radical amount over Nb_2O_5 .

amount of the radical species drastically decreases on going from 0 to 4 mol % Nb_2O_5 loading. This change becomes gradual at loadings over 4 mol %. Thus, these results demonstrate that the surface coverage of TiO_2 with Nb_2O_5 effectively inhibits the formation of oxygen anion radicals. In particular, the generation of O_3^- was completely inhibited by full coverage (Scheme 2). The g values of the ESR signal assigned to O_2^- , as generated on 5 mol % $\text{Nb}_2\text{O}_5/\text{TiO}_2$, are different from those on TT- Nb_2O_5 . This may be due to the

Scheme 2. Plausible Surface Species on the Nb₂O₅/TiO₂: (a) below 3 mol % Nb₂O₅ Loading and (b) over the Monolayer



differences in crystallinity of Nb₂O₅ (amorphous or TT-phase). The ESR spectrum of the oxygen anion radicals formed on 5 mol % Nb₂O₅/TiO₂ has a shoulder feature in the region of $g = 2.003\text{--}2.008$. This is in good agreement with the peak features of O₂⁻, formed on TT-Nb₂O₅ in the same region (Supporting Information Figure S5), which implies the formation of O₂⁻ on TT-Nb₂O₅ (Scheme 2).

In addition to the signals of the oxygen anion radicals, small signals were also observed in the region of $g < 2.000$. These can be assigned to excited electrons trapped by the Ti⁴⁺ sites (equivalent to Ti³⁺) and are composed of two distinct signals (Ti³⁺ (i) and (ii)). The g values of Ti³⁺ (i) ($g_1 = 1.982$, $g_2 = 1.977$, $g_3 = 1.971$) are similar to those for bulk and surface Ti³⁺ in TiO₂.⁴¹ The g values and the signal intensity do not depend on the loading amount of Nb₂O₅. These suggest that the Ti³⁺ (i) corresponds to the bulk Ti³⁺ site. On the other hand, the signals assigned to Ti³⁺ (ii) are only observed with a large surface coverage of TiO₂ (>3 mol %). The g values of Ti³⁺ (ii) ($g_1 = 1.990$, $g_{ii} = 1.962$) are almost identical to those obtained from Nb-doped anatase TiO₂ and are attributed to the interstitial Ti³⁺ ion.^{42,43} On this basis, the Ti³⁺ (ii) is assignable to the interfacial Ti³⁺ sites adjacent to loaded Nb₂O₅ (Scheme 2).

Photocatalytic Activity and Selectivity. The photocatalytic activities and selectivities of the TiO₂, Nb₂O₅/TiO₂, and Nb₂O₅ catalysts were evaluated using the photooxidation of 1-pentanol, as shown in Figure 5. Although the photocatalytic activity gradually decreases as the loading of Nb₂O₅ is increased, 5 mol % Nb₂O₅/TiO₂, which seems to be fully covered with Nb₂O₅, still exhibits a higher activity than Nb₂O₅. If the excited electrons or positive holes generated in the inner TiO₂ core cannot be transferred to the surface Nb₂O₅ thin layer, the photocatalytic activity of the fully covered Nb₂O₅/TiO₂ catalyst (>4 mol % loading) should be lower than that of bare Nb₂O₅. Therefore, the photogenerated charge carriers due to band gap excitation of the inner TiO₂ core can be transferred to the catalyst surface and used for the alcohol oxidation.

The selectivity to partial oxidation products became higher on going from 1 to 5 mol % loading and reached 97%, which is as high as that obtained with Nb₂O₅ (Figure 5a). The higher selectivities of the Nb₂O₅/TiO₂ catalysts, as compared with the TiO₂, are maintained at the same conversion level (Figure 5b). Thus, the surface coverage of TiO₂ with Nb₂O₅ effectively enhances the selectivity of the photooxidation of 1-pentanol. The selectivity at comparable conversion levels increased with increasing Nb₂O₅ loading up to 3 mol %.

As mentioned above, the ESR study revealed that coverage of the TiO₂ surface with Nb₂O₅ inhibits the generation of O₃⁻, which is highly active toward the complete oxidation of organic molecules. In fact, O₃⁻ is known to be active even at room temperature, whereas O₂⁻ is stable up to ca. 423 K. On this basis, the change in selectivity on going from 0 to 3 mol %

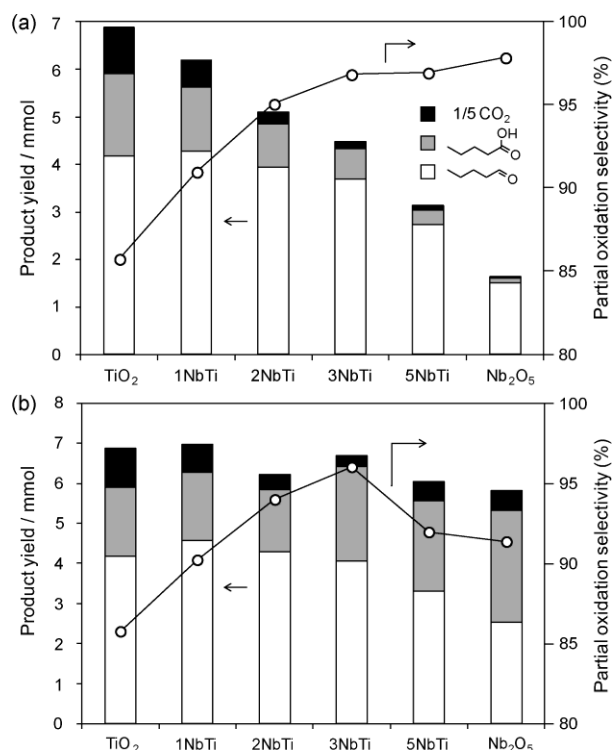


Figure 5. Product yields in the photooxidation of 1-pentanol over TiO₂, n mol % Nb₂O₅/TiO₂ (abbreviated as n NbTi; $n = 1, 2, 3$, and 5) and Nb₂O₅; (a) after 5 h of photo irradiation, (b) at a comparable conversion level (TiO₂; 5 h, 1NbTi; 5.5 h, 2NbTi; 6 h, 3NbTi; 7.5 h, 5NbTi; 13 h and Nb₂O₅; 20 h).

Nb₂O₅ loading agrees with the results from the ESR study. However, 5 mol % Nb₂O₅/TiO₂ and Nb₂O₅ showed lower selectivities compared with 3 mol %. In this case, higher yields of pentanoic acid are obtained than the lower loading homologues. This indicates that overoxidation of the products to CO₂ takes place more severely for 5 mol % Nb₂O₅/TiO₂ and Nb₂O₅ due to the much longer reaction times. Figure 6 shows

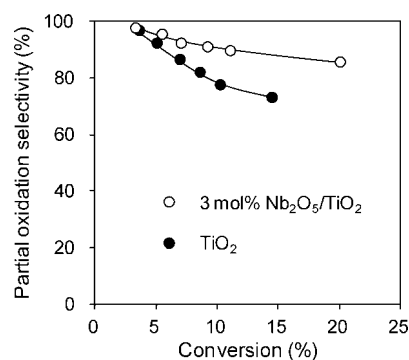


Figure 6. Selectivity-conversion plots for the photooxidation of 1-pentanol over 3 mol % Nb₂O₅/TiO₂ and TiO₂.

the relationship between selectivity and conversion in the photooxidation of 1-pentanol over 3 mol % Nb₂O₅/TiO₂ and TiO₂. At the higher conversion level, 3 mol % Nb₂O₅/TiO₂ catalyst exhibited a much higher selectivity than TiO₂. The 3 mol % Nb₂O₅/TiO₂ catalyst maintained more than 85% selectivity, even at 20% conversion. However, the selectivity fell below 75% at 15% conversion when TiO₂ was used.

We went on to apply 3 mol % Nb₂O₅/TiO₂ to the oxidation of various alcohols. The activities and selectivities were compared with those of TiO₂ and Nb₂O₅ (Supporting Information Figure S6). The oxidation of several secondary alcohols (2-pentanol, 3-pentanol, cyclohexanol) gave the corresponding ketones and certain amounts of CO₂. In each case, the 3 mol % Nb₂O₅/TiO₂ catalyst showed not only a much higher activity than Nb₂O₅ without lowering selectivity, but also a higher selectivity than TiO₂ at a comparable conversion level. Thus, the surface coverage of TiO₂ with Nb₂O₅ enhanced the selective partial oxidation of various alcohols, including primary and secondary alcohols.

CONCLUSIONS

In this study, we prepared a series of TiO₂ supported Nb₂O₅ catalysts (Nb₂O₅/TiO₂, with loadings of Nb₂O₅ between 0–5 mol %) for the selective photooxidation of alcohols. XPS studies suggested that the TiO₂ surface was completely covered with Nb₂O₅ at loadings over 3.5 mol %. UV–vis spectra of TiO₂ and a series of Nb₂O₅/TiO₂ samples revealed that the absorption band of the catalyst remained unchanged by the addition of Nb₂O₅; however, the amounts of photogenerated O₂^{•-} and O₃^{•-} over the catalyst were estimated by ESR to be drastically decreased with increased loadings of Nb₂O₅. In particular, O₃^{•-}, which can be formed on anatase TiO₂, completely disappeared at loadings over 4 mol %. We also investigated the photocatalytic activities and selectivities of these catalysts in the oxidation of 1-pentanol. Although the photocatalytic activity gradually decreased with increasing of Nb₂O₅ loading, the selectivity was enhanced. At a comparable conversion level, the maximum selectivity was obtained with a 3 mol % Nb₂O₅ loading. Similarly, 3 mol % Nb₂O₅/TiO₂ exhibited higher selectivities than TiO₂ in the oxidation of secondary alcohols (2-pentanol, 3-pentanol, and cyclohexanol). Thus, the surface coverage of TiO₂ with Nb₂O₅ effectively enhanced the selectivity to partial oxidation product(s) in alcohol photooxidation, due to inhibition of O₃^{•-} formation. Furthermore, the present study proves the strategy to inhibit the formation of active oxygen species effective and provides a new promising basis for selective oxidation using TiO₂-based photocatalysts.

ASSOCIATED CONTENT

Supporting Information

Setup of reactor, XPS, UV–vis spectra, surface areas of catalysts, ESR spectra, and substrate scope. This material is available free of charge via the Internet at <http://pubs.acs.org>.

AUTHOR INFORMATION

Corresponding Author

*Phone: +81-75-383-2558. Fax: +81-75-383-2561. E-mail: (T.S.) shishido@moleng.kyoto-u.ac.jp, (T.T.) tanakat@moleng.kyoto-u.ac.jp.

ACKNOWLEDGMENTS

S.F. thanks the JSPS Research Fellowships for Young Scientists.

REFERENCES

- (1) Fox, M. A.; Dulay, M. T. *Chem. Rev.* **1993**, *93*, 341–357.
- (2) Mills, A.; LeHunte, S. J. *Photochem. Photobiol. A* **1997**, *108*, 1–35.
- (3) Maldotti, A.; Molinari, A.; Amadelli, R. *Chem. Rev.* **2002**, *102*, 3811–3836.
- (4) Mu, W.; Herrmann, J. M.; Pichat, P. *Catal. Lett.* **1989**, *3*, 73–84.
- (5) Boarini, P.; Carassiti, V.; Maldotti, A.; Amadelli, R. *Langmuir* **1998**, *14*, 2080–2085.
- (6) Almquist, C. B.; Biswas, P. *Appl. Catal., A* **2001**, *214*, 259–271.
- (7) Du, P.; Moulijn, J. A.; Mul, G. J. *Catal.* **2006**, *238*, 342–352.
- (8) Pillai, U. R.; Sahle-Demessie, E. J. *Catal.* **2002**, *211*, 434–444.
- (9) Augugliaro, V.; Caronna, T.; Loddo, V.; Marci, G.; Palmisano, G.; Palmisano, L.; Yurdakal, S. *Chem.—Eur. J.* **2008**, *14*, 4640–4646.
- (10) Yurdakal, S.; Palmisano, G.; Loddo, V.; Augugliaro, V.; Palmisano, L. *J. Am. Chem. Soc.* **2008**, *130*, 1568–1569.
- (11) Yurdakal, S.; Palmisano, G.; Loddo, V.; Alagoz, O.; Augugliaro, V.; Palmisano, L. *Green Chem.* **2009**, *11*, 510–516.
- (12) Zhang, M.; Wang, Q.; Chen, C. C.; Zang, L.; Ma, W. H.; Zhao, J. C. *Angew. Chem., Int. Ed.* **2009**, *48*, 6081–6084.
- (13) Wang, Q.; Zhang, M. A.; Chen, C. C.; Ma, W. H.; Zhao, J. C. *Angew. Chem., Int. Ed.* **2010**, *49*, 7976–7979.
- (14) Yurdakal, S.; Loddo, V.; Palmisano, G.; Augugliaro, V.; Berber, H.; Palmisano, L. *Ind. Eng. Chem. Res.* **2010**, *49*, 6699–6708.
- (15) Augugliaro, V.; Palmisano, L. *ChemSusChem* **2010**, *3*, 1135–1138.
- (16) Aika, K. I.; Lunsford, J. H. *J. Phys. Chem.* **1978**, *82*, 1794–1800.
- (17) Furube, A.; Tamaki, Y.; Murai, M.; Hara, K.; Katoh, R.; Tachiya, M. *J. Am. Chem. Soc.* **2006**, *128*, 416–417.
- (18) Takita, Y.; Lunsford, J. H. *J. Phys. Chem.* **1979**, *83*, 683–688.
- (19) Takita, Y.; Iwamoto, M.; Lunsford, J. H. *J. Phys. Chem.* **1980**, *84*, 1710–1712.
- (20) Lunsford, J. H. *Catal. Rev.* **1973**, *8*, 135–157.
- (21) Anpo, M. *Bull. Chem. Soc. Jpn.* **2004**, *77*, 1427–1442.
- (22) Tsukamoto, D.; Ikeda, M.; Shiraishi, Y.; Hara, T.; Ichikuni, N.; Tanaka, S.; Hirai, T. *Chem.—Eur. J.* **2011**, *17*, 9816–9824.
- (23) Ohuchi, T.; Miyatake, T.; Hitomi, Y.; Tanaka, T. *Catal. Today* **2007**, *120*, 233–239.
- (24) Shishido, T.; Miyatake, T.; Teramura, K.; Hitomi, Y.; Yamashita, H.; Tanaka, T. *J. Phys. Chem. C* **2009**, *113*, 18713–18718.
- (25) Furukawa, S.; Tamura, A.; Shishido, T.; Teramura, K.; Tanaka, T. *Appl. Catal., B* **2011**, *110*, 216–220.
- (26) Furukawa, S.; Ohno, Y.; Shishido, T.; Teramura, K.; Tanaka, T. *ChemPhysChem* **2011**, *12*, 2823–2830.
- (27) Jehng, J. M.; Wachs, I. E. *J. Mol. Catal.* **1991**, *67*, 369–387.
- (28) Ko, E. I.; Weissman, J. G. *Catal. Today* **1990**, *8*, 27–36.
- (29) Tamura, S.; Kato, K.; Goto, M. *Z. Anorg. Allg. Chem.* **1974**, *410*, 313–315.
- (30) Tamura, S. *J. Mater. Sci.* **1972**, *7*, 298–302.
- (31) Frevel, L. K.; Rinn, H. W. *Anal. Chem.* **1955**, *27*, 1329–1330.
- (32) Pittman, R. M.; Bell, A. T. *J. Phys. Chem.* **1993**, *97*, 12178–12185.
- (33) Tsur, Y.; Simakov, D. S. A. *J. Nanopart. Res.* **2008**, *10*, 77–85.
- (34) Okumura, M.; Coronado, J. M.; Soria, J.; Haruta, M.; Conesa, J. C. *J. Catal.* **2001**, *203*, 168–174.
- (35) Meriaudeau, P.; Vedrine, J. C. *J. Chem. Soc., Faraday Trans. 2* **1976**, *72*, 472–480.
- (36) Yamazoe, S.; Okumura, T.; Tanaka, T. *Catal. Today* **2007**, *120*, 220–225.
- (37) Tench, A. J. *J. Chem. Soc., Faraday Trans. 1* **1972**, *68*, 1181–1189.
- (38) Wong, N. B.; Lunsford, J. H. *J. Chem. Phys.* **1972**, *56*, 2664–2667.
- (39) Einaga, H.; Ogata, A.; Futamura, S.; Ibusuki, T. *Chem. Phys. Lett.* **2001**, *338*, 303–307.
- (40) Gonzalez-Elipse, A. R.; Munuera, G.; Soria, J. *J. Chem. Soc., Faraday Trans. 1* **1979**, *75*, 748–761.
- (41) Murphy, D. M.; Attwood, A. L.; Edwards, J. L.; Egerton, T. A.; Harrison, R. W. *Res. Chem. Intermed.* **2003**, *29*, 449–465.
- (42) Kiwi, J.; Suss, J. T.; Szapiro, S. *Chem. Phys. Lett.* **1984**, *106*, 135–138.
- (43) Nosaka, Y.; Nakaoka, Y. *J. Photochem. Photobiol. A* **1997**, *110*, 299–305.